54

Forest Biomass Carbon Stocks and Fluxes in a Broader Context

Insights and Opportunities Associated with the Central Panama Plot Network

Helene C. Muller-Landau,[1]* *Camille Piponiot,*[2] *Rolando Pérez,*[1] *Salomón Aguilar,*[1] *Suzanne Lao,*[1] *David Mitre,*[1] *and Richard Condit*[3]

ABSTRACT. Comparisons among sites varying in climate and soils can yield important insights into the mechanisms shaping forest carbon stocks and fluxes. Research at a network of small plots spanning regional variation in central Panama, including a strong regional rainfall gradient and high geological heterogeneity, provides excellent opportunities for such comparisons, and places findings for Barro Colorado Island (BCI) in a broader context. Here, we examine regional variation in climate, soils, and land use history and discuss associated datasets. We then review previous work and present updated analyses of among-plot variation in aboveground biomass, aboveground woody productivity, and tree mortality rates with dry-season severity and soil fertility. We enumerate the different types of complementary datasets that have been collected in subsets of these plots, which offer opportunities to investigate alternative hypotheses regarding underlying mechanisms, and close with a discussion of promising directions for future research.

Keywords: aboveground biomass; aboveground woody productivity; tree mortality; precipitation gradient; soil fertility; geological variation; tree census; phosphorus

INTRODUCTION

Tropical forests vary widely in their aboveground biomass (AGB, mass per area), as well as in their woody productivity and other carbon stocks and fluxes, even after controlling for stand age (Cleveland et al., 2011; Xu et al., 2021). AGB depends proximally on aboveground woody productivity (AWP, mass per area per time) and aboveground woody residence time, the average time that an atom of carbon remains in AGB before it becomes dead wood (Muller-Landau et al., 2021). AWP is the production of woody AGB by tree growth and recruitment, which can be calculated from plot re-census data with appropriate correction for census interval length (Kohyama et al., 2018). Woody residence time depends (negatively) on tree mortality rates, especially of the largest trees. All else equal, higher AWP leads to higher AGB, and higher tree mortality rate leads to lower woody residence time and lower AGB. Comparisons among sites varying in climate, soils, and other factors have helped illuminate the mechanisms underlying variation in AGB, AWP, and other carbon stocks and fluxes (Cleveland et al., 2011; Muller-Landau et al., 2021).

---

[1] Smithsonian Tropical Research Institute, P.O. Box 0843-03092, Balboa, Ancón, Republic of Panama.

[2] UR Forests and Societies, Cirad, Université de Montpellier, Montpellier 34000, France.

[3] Now retired, author R.C. is an independent researcher.

* Correspondence: mullerh@si.edu

Muller-Landau, https://orcid.org/0000-0002-3526-9021

Piponiot, https://orcid.org/0000-0002-3473-1982

Lao, https://orcid.org/0009-0006-4525-9376

Condit, https://orcid.org/0000-0003-4191-1495

Manuscript received 14 November 2022; accepted 17 July 2023.

Panama provides excellent opportunities for investigating how forest carbon stocks and fluxes vary with environmental drivers, and the regional perspective places values for Barro Colorado Island (BCI) and the Barro Colorado Nature Monument (BCNM) in a larger context. Central Panama features high heterogeneity in geology and soils and a steep regional rainfall gradient from the drier Pacific side to the wetter Caribbean side of the isthmus (2,000–4,000 mm annual precipitation; dry-season length varying three to five months). In the late 1990s, Rick Condit established 46 forest census plots spanning this regional variation in climate and soils, including the 4-ha Cocoli and 5.96-ha San Lorenzo (formerly Sherman) large plots, 34 1-ha plots and 10 0.32-ha plots (Condit et al., 2001; Condit et al., 2013; Condit, 2024). An additional 21 1-ha plots were established later (mostly in drier forests and outside the canal watershed), for a total of 67 plots, although some plots have been lost to land use change or access restrictions. A set of 94 small (0.1 ha) plots at Smithsonian Tropical Research Institute's (STRI's) Agua Salud site provides an additional reference for young secondary forests (van Breugel et al., 2019). Elsewhere in Panama, there are plots at higher elevation in western Panama (Dalling and Turner, 2021), in mangroves (Wang et al., 2004), and in the Darien (Mateo-Vega et al., 2019).

In this chapter, we focus on what the central Panama plots can tell us about patterns and mechanisms of variation in aboveground forest carbon stocks and fluxes in relation to climate and soils. We first review environmental variation among the plots and how it has been characterized. We then evaluate among-plot variation in AGB, AWP, and tree mortality rates, including new analyses and a review of previously published studies. We close with recommendations for future research. Elsewhere in this volume, Condit (2024) addresses how the tree species compositional information from these plots has shaped our understanding of the BCI tree community, and Cusack (2024) reviews patterns of variation in soil carbon stocks and fluxes across these plots.

REGIONAL VARIATION IN CLIMATE, SOIL, AND LAND USE HISTORY

Sites in central Panama vary strongly in total annual rainfall and in the severity of the dry season, and hardly at all in temperature (Fig. 1). Seasonal climate variation in this region is governed by the movements of the Inter Tropical Convergence Zone (ITCZ), a band of clouds at the thermal equator. The wet season extends approximately from May through December, when the ITCZ is overhead. The single dry season, from December/January to March/April, occurs when the ITCZ is to the south, and ranges three to five months regionally (compared with a range of zero to six months across tropical forests globally).

Historic rainfall patterns in this region are well documented at many ground stations, in large part because of the importance of rainfall for the operation of the Panama Canal. Condit estimated plot-specific climate variables by fitting spatial models to these ground station data. The resulting estimates have improved over time as the number of rainfall stations incorporated increased, modeling methods improved, and the modeled response variables have shifted to more biologically relevant metrics, from total annual rainfall and total dry-season rainfall (Pyke et al., 2001) to dry-season length (Engelbrecht et al., 2007) to maximum cumulative moisture deficit (Condit et al., 2013). Maximum cumulative moisture deficit provides a measure of dry-season severity. It is calculated as the maximum cumulative (between any two days of the year) deficit of precipitation relative to potential evapotranspiration. Given the absence of site-specific potential evapotranspiration data, Condit et al. (2013) employed values based on measurements at BCI, with a correction for elevational differences.

Gridded global climate reanalysis datasets informed by satellite and ground-based climate data and mechanistic models now provide additional options for visualizing landscape-level patterns in climate, or rather, estimated climate (Fig. 1). Mean annual precipitation in the CHELSA 2.1 climatologies for 1981–2010 (Karger et al., 2017, 2018) is well-correlated with ground measurements across sites in central Panama ($n = 71$, $r = 0.70$), although it averages 289 mm higher, and systematically underestimates rainfall at the wettest sites (Fig. S1). Maximum climatological water deficit (MCWD) calculated from mean monthly rainfall and monthly potential evapotranspiration data from CHELSA v. 2.1 is well-correlated with those modeled for forest inventory sites by Condit ($n = 77$, $r = 0.71$), although on average 186 mm higher (Fig. S2).

Central Panama is also geologically heterogeneous, and this together with the variation in climate leads to strong variation in soil nutrient availability (Condit et al., 2013). Regional geology was well mapped due to its importance for canal construction (Woodring et al., 1980), and thus the geological formations underlying plots were known prior to plot establishment. Detailed soil chemistry data were collected at 77 plots and inventory sites in the regional network (Turner and Condit, 2022), in addition to more detailed studies in the BCNM and Agua Salud. Condit et al. (2013) selected a set of seven variables that were relatively weakly correlated to represent soils variation across the sites: resin phosphorus (a measure of readily exchangeable phosphorus, extracted with anion-exchange resin), calcium, potassium, aluminum, iron, zinc, and inorganic nitrogen. Resin phosphorus was the most important soils variable in explaining tree species distributions (Condit et al., 2013) and ranged over 100-fold from 0.07 to 22.8 mg kg^{-1} among the central Panama sites.

The plot network established by Condit spans regional variation in climate and soils within forested areas, which itself spans a substantial fraction of the range found globally across tropical forests (Fig. 2). The high local geological heterogeneity means there is a wide range of soil fertility for any given dry-season severity. However, dry-season severity and soil fertility do not vary completely independently; wetter sites tend to have lower fertility soils. Furthermore, soils differ in their water-holding capacity and other characteristics that affect plant-available moisture, beyond the influences of climate alone. For example,

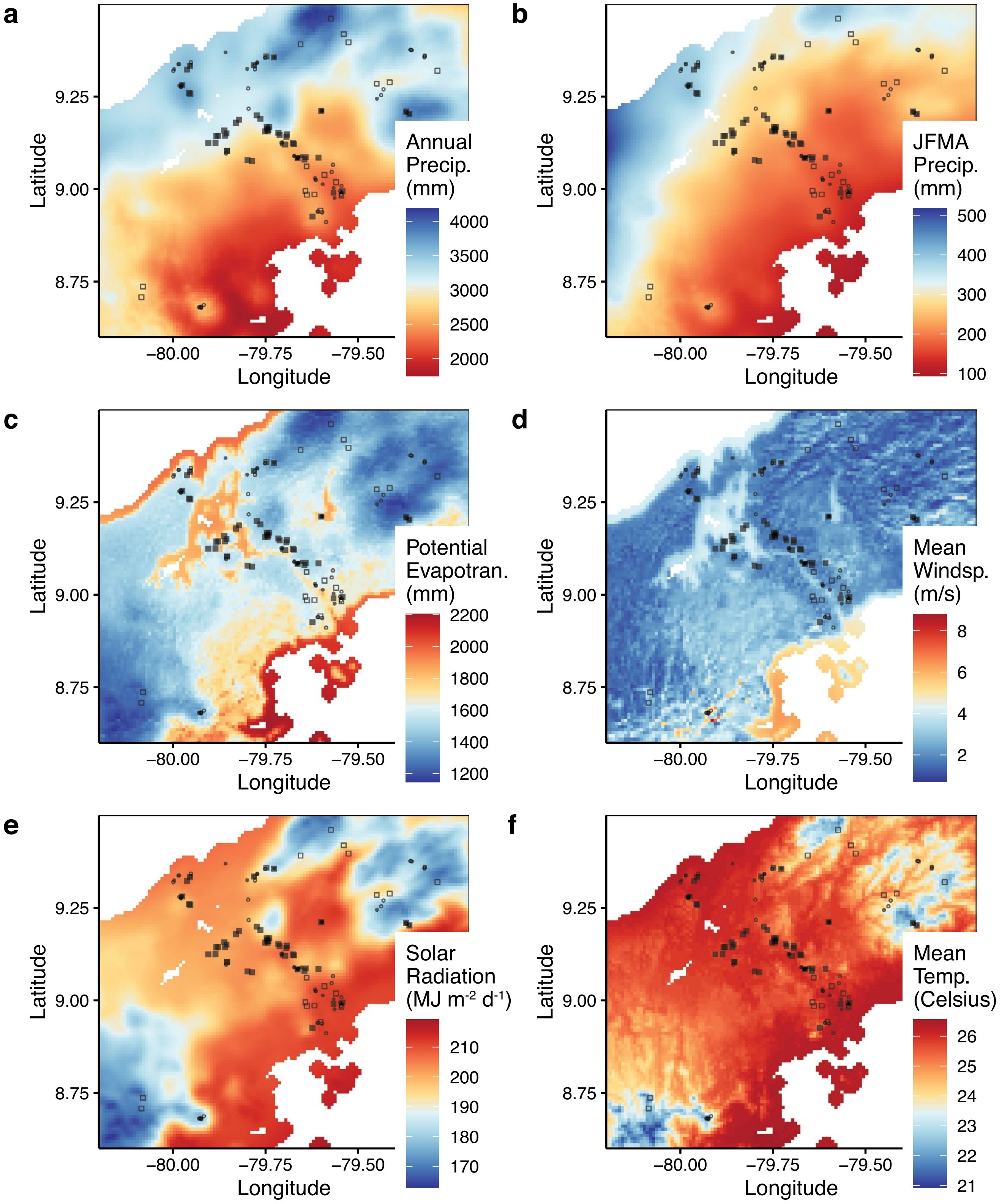

FIGURE 1. Spatial variation in central Panama in (**a**) estimated mean annual precipitation (mm), (**b**) mean precipitation for January to April (mm), (**c**) mean annual potential evapotranspiration (mm), (**d**) near-surface wind speed (m s^{-1}), (**e**) mean daily solar radiation specifically surface downwelling shortwave flux (MJ m^{-2} d^{-1}), and (**f**) mean annual temperature (°C), from the CHELSA v. 2.1 average climatologies for 1981–2010 (Karger et al., 2017, 2018), together with the locations of forest plots with soils data (filled squares), forest plots lacking soil data (open squares), onetime inventories with soils data (filled circles), and onetime inventories lacking soils data (open circles).

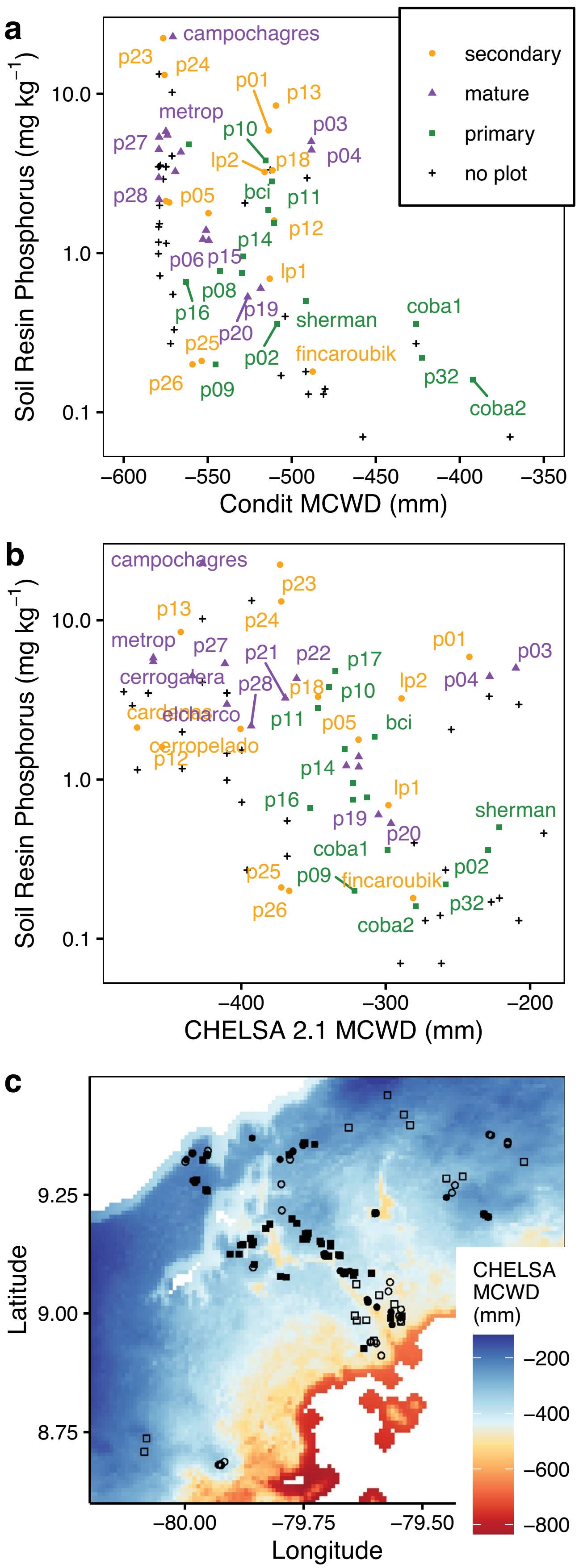

FIGURE 2. Among-site variation in soil phosphorus and maximum climatological water deficit (MCWD), with MCWD calculated either (**a**) from spatial modeling of ground-based precipitation data by Condit, or (**b, c**) from the monthly CHELSA 2.1 climatology. Forest plots (p) with soils data (n = 45) are shown in panels (a) and (b) with labels and colored symbols indicating stand-age class (secondary is youngest, mature is intermediate, and primary is oldest) and in panel (c) with filled diamonds. Onetime inventory sites with soils data (n = 32) are shown with black crosses (all panels); plots without soils data as open diamonds and inventory sites without soils data as small points (c). The Barro Colorado National Monument sites are p10, p14, and BCI (Barro Colorado Island 50-ha plot), on BCI; p11 and p18 on the Peña Blanca Peninsula; gigante1 and gigante2 on the Gigante Peninsula; and p12 and p13 on the Bohio Peninsula. Other abbreviations are explained in Table 1.

soils on the Tau Formation (limestone) dry out faster in the dry season, and forests on these soils have higher abundances of deciduous species than expected based on their rainfall (Bohlman, 2010). The BCNM sites are mostly intermediate in soil fertility and dry-season severity relative to the region (see Fig. 2 caption). The range of soil resin phosphorus across 77 Panama plots was larger than that found across 71 Amazonian plots (1.30 to 21.82 mg kg^{-1}) by Quesada et al. (2010). (The Amazon data are for 0-30 cm soil depth compared with 0-10 cm for Panama; given that phosphorus declines with depth, this suggests a comparison at constant depth would show an even greater range difference.)

Land use history is confounded with climate and soils in central Panama, as in most regions, reflecting greater forest conversion in drier, flatter, and more fertile sites. Indeed, there are no old-growth forests on the drier Pacific side of the isthmus. Each of the central Panama plots has been classified by expert local botanists as secondary (the youngest class), mature (intermediate), or primary (oldest), enabling stand-age class to be included as a categorical variable (Chave et al., 2004), although these classifications are inherently uncertain.

INSIGHT INTO REGIONAL VARIATION IN FOREST CARBON STOCKS AND FLUXES

Estimated AGB varies almost threefold among the central Panama plots, and some of this variation is explained by climate, soils, and forest age class. A multiple regression of log-transformed AGB against Condit's MCWD and log-transformed resin soil phosphorus in 45 plots shows a significant increase (p = 0.006) from dry to wet sites and a significant positive effect of soil phosphorus (p = 0.049) (adjusted r^2 = 0.14; Fig. 3a,b). By comparison, Turner et al. (2018) found a significant positive effect of MCWD and no effect of soil phosphorus for untransformed AGB in 32 of these plots, and qualitatively the same result was previously reported by Chave et al. (2004) based on an analysis of variance (ANOVA) of 49 central Panama plots or subplots in relation to annual precipitation, dry-season length, stand-age class, and geology (10 levels).

Estimated AWP varies more than twofold among the plots but shows only weak and nonsignificant relationships with environmental variables. A multiple regression of log-transformed AWP against MCWD and log-transformed soil phosphorus in 39 plots shows a nonsignificant increase from dry to wet sites, and nonsignificant decrease with soil phosphorus (Fig. 3c,d). Considering that AWP and AGB show similar patterns with MCWD and soils, it's not surprising that Turner et al. (2018) found that relative AGB growth, defined as AWP/AGB, was not related to MCWD or soil phosphorus in a multiple regression (n = 32 plots). Tree diameter growth was higher in wetter sites for small trees, but not large trees, and increased with plot resin phosphorus after controlling for tree size and species; however, plot-level mean growth rates did not vary with phosphorus (Turner et al., 2018).

The increasing trends of AGB and AWP from drier to wetter sites in central Panama are broadly consistent with those for other tropical forests. Productivity and biomass increase from dry to wet forests because of both direct effects of limited water availability on productivity as well as shifts in functional composition (Muller-Landau et al., 2021).

In contrast, the trend for a negative relationship of AWP with soil phosphorus is unexpected. Most tropical forest studies have found positive relationships of woody productivity with soil fertility in general and phosphorus in particular (Muller-Landau et al., 2021). An increase in productivity with soil fertility is also predicted by mechanistic models in which higher nutrient availability reduces the cost of acquiring nutrients and enables plants to achieve greater light use efficiency and thus faster growth rates. A nutrient fertilization experiment in the BCNM found no effect on AWP, however, in contrast to significant positive effects on litterfall and reproduction (chapter 60, Wright et al., 2024), and a meta-analysis of experimental nutrient addition in tropical forests found positive effects on tree diameter growth rates in secondary forests but not old-growth forests (Wright et al., 2018). In combination, these results suggest that total net primary productivity (NPP, total plant biomass production) increases at more fertile sites in the region but that this is not translating into higher AWP because of allocational shifts. Increased consumption by herbivores, compositional shifts toward lianas, and confounded variation in soil water-holding capacity, topography, and stand age may also play a role—possibilities that remain to be tested.

Tree mortality rates vary almost threefold among the sites in central Panama and decline significantly with MCWD and soil phosphorus (Fig. 3e,f). There have been relatively few studies of among-site variation in tree mortality rates in tropical forests, and few of those have found strong or statistically significant effects (Muller-Landau et al., 2021). Weak relationships for mortality rates in part reflect high sampling errors for this binomial variable in individual plots, especially considering high temporal variation and spatial clustering in mortality events. They also likely reflect biological reality, given that there is little mechanistic basis for expecting climate or soils to be strongly predictive of tree mortality rates (McDowell et al., 2018). In the available studies, mortality tends to decrease in wetter forests (consistent with the pattern here) and increase with soil fertility (contrary to the pattern here) more often than not. Although the Panama sites are unusual in their patterns of AWP and mortality rate with soil fertility, the lack of a relationship of AGB with soil fertility is unexceptional. Studies are fairly evenly split between increasing, decreasing, and no relationships for AGB with fertility, a pattern that can be explained by contrasting influences and strengths of patterns with AWP and mortality rate (Muller-Landau et al., 2021).

The directions of trends in among-site variation in AGB, AWP, and tree mortality rate are robust to the details of the analyses (compare Fig. 3 with Fig. S3, S4, and see "Online Supplemental Materials" section). Whether trends are statistically significant, however, is sensitive to these details. Of the variables considered here, AWP is the most sensitive to methodological details, in particular including the thresholds used to identify erroneous values and the methods for substituting for them (Muller-Landau et al., 2014). Models including stand-age class performed more poorly (higher AICc) than those omitting this term for all response variables. The regressions for AWP and mortality are strongly influenced by the three highest-elevation sites (p32, coba1, and coba2 at 363, 515, and 643 m elevation), which also are the wettest according to the Condit MCWD but not the CHELSA MCWD. If these sites are omitted, then multiple regressions find significant effects of phosphorus on AGB (positive) and mortality (negative), no significant effect of phosphorus on AWP, and no significant effects of MCWD, regardless of which MCWD metric is used (Appendix S1).

CONCLUSIONS AND FUTURE DIRECTIONS

Strong regional variation in rainfall and geology in central Panama offers an excellent opportunity to investigate variation in tropical forests with climate and soils. The tree census data collected in the regional small plot network have enabled important analyses of forest structure, dynamics, and composition as well as aboveground woody carbon stocks and fluxes (Condit et al., 2002; Chave et al., 2004; Engelbrecht et al., 2007; Condit et al., 2013; Turner et al., 2018). The value of these plots will be further enhanced by continued maintenance of the core census data, expansion of the plot network to more completely represent regional environmental conditions, and the elucidation of disturbance histories of the plots and the landscape. They are a resource not only for ground-based studies but also for calibration and validation of remote sensing studies, and in turn, remote sensing increasingly offers important information about environmental variables, forest structure, and function

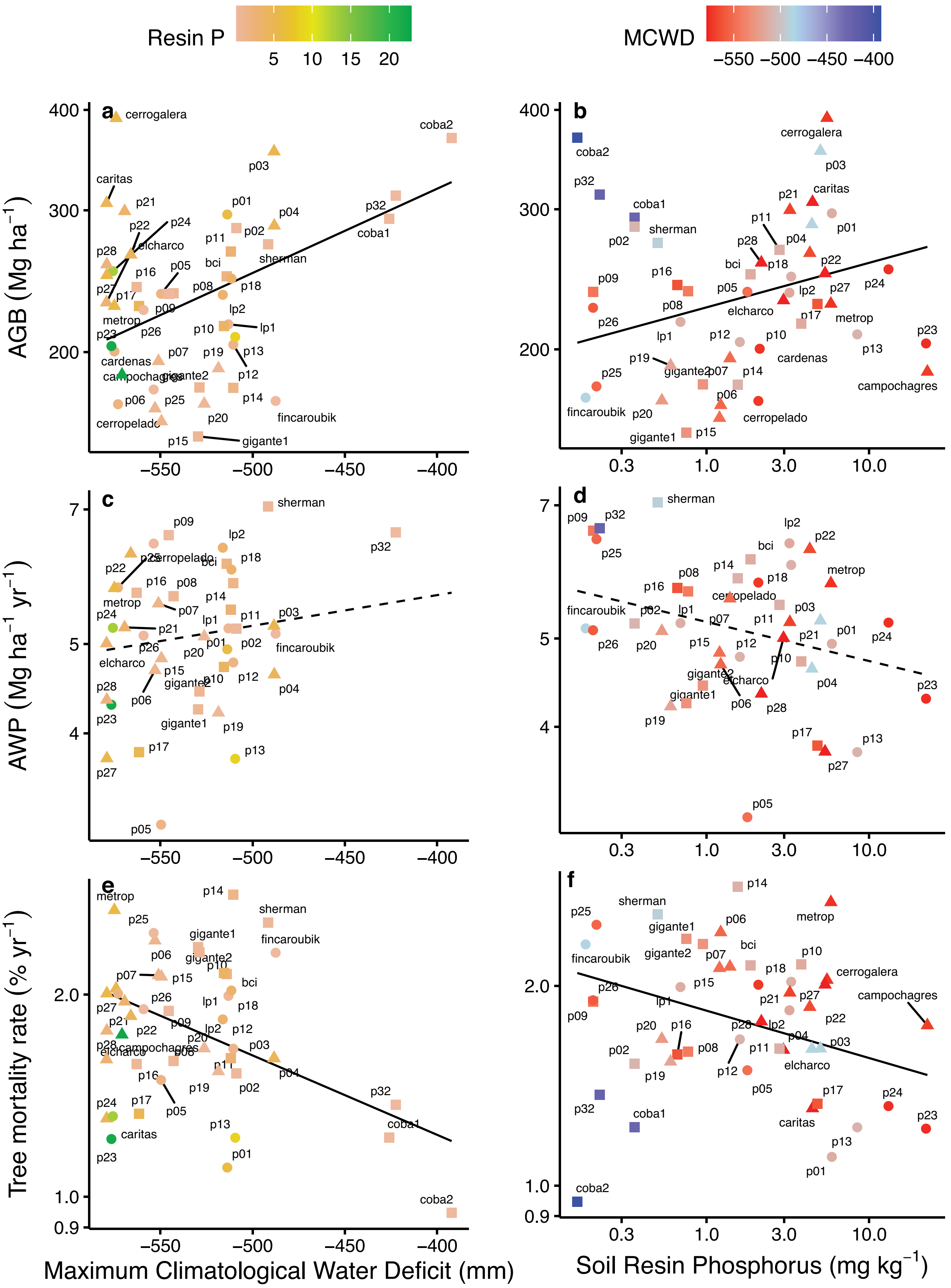

Resin P
5
10
15
20
MCWD
−550
−500
−450
−400
a
AGB (Mg ha^{-1})
400
300
200
cerrogalera
coba2
p03
caritas
p21
p01
p04
p32
p24
p22
p02
coba1
p11
elcharco
p28
sherman
bci
p16
p05
p27
p17
p08
p18
p09
metrop
lp2
p23
p26
p10
lp1
cardenas
p07
p19
p13
campochagres
gigante2
p12
p06
p25
p14
cerropelado
p20
fincaroubik
p15
gigante1
−550
−500
−450
−400
b
400
300
200
coba2
cerrogalera
p03
p32
caritas
p21
coba1
p11
p01
sherman
p02
p28
p04
p22
bci
p18
p16
p09
p05
lp2
p27
p24
p08
elcharco
p17
metrop
p26
lp1
p12
p10
p23
p13
cardenas
p19
gigante2
p07
p14
p25
campochagres
p06
fincaroubik
p20
cerropelado
gigante1
p15
0.3
1.0
3.0
10.0
c
AWP (Mg ha^{-1} yr^{-1})
7
5
4
sherman
p09
p32
lp2
p25
cerropelado
p18
p22
bci
p16
p08
p14
metrop
p07
p24
lp1
p11
p03
p21
p26
p01
p02
fincaroubik
p20
elcharco
p15
p10
p12
p28
gigante2
p04
p06
p23
gigante1
p19
p17
p13
p27
p05
−550
−500
−450
−400
d
7
5
4
sherman
p09
p32
lp2
p22
p25
bci
p14
metrop
p08
p18
p16
cerropelado
fincaroubik
p02
lp1
p03
p07
p11
p01
p26
p20
p15
p12
p21
p24
p10
gigante2
elcharco
p04
gigante1
p06
p23
p28
p19
p17
p13
p27
p05
0.3
1.0
3.0
10.0
e
Tree mortality rate (% yr^{-1})
2.0
1.0
0.9
metrop
p14
p25
sherman
gigante1
fincaroubik
p06
gigante2
p10
p07
p15
bci
p26
p27
lp1
p18
p21
p09
p22
p20
lp2
p12
p28
campochagres
elcharco
p08
p03
p11
p04
p16
p19
p02
p32
p24
p17
p05
p13
coba1
caritas
p23
p01
coba2
−550
−500
−450
−400
Maximum Climatological Water Deficit (mm)
f
2.0
1.0
0.9
p14
sherman
metrop
p25
gigante1
p06
bci
fincaroubik
gigante2
p07
p10
p18
cerrogalera
p15
p26
lp1
p21
p27
campochagres
p09
p22
p20
p16
p28
lp2
p04
p02
p08
p11
p03
p12
elcharco
p19
p05
p17
p24
p32
coba1
caritas
p23
p13
p01
coba2
0.3
1.0
3.0
10.0
Soil Resin Phosphorus (mg kg^{-1})

FIGURE 3. (*Opposite*) Among-plot relationships of (top) aboveground biomass (AGB), (middle) aboveground woody productivity (AWP), and (bottom) tree mortality rate to (left) maximum climatological moisture deficit (MCWD, mm) and (right) soil resin phosphorus (resin P, mg kg^{-1}) with fitted lines based on a multiple regression against these two variables and their associated *p*-values (solid lines indicate $p < 0.05$; dashed lines indicated $p > 0.05$). AGB and AWP were calculated from trunk diameter and taxon-specific wood density using allometric equations incorporating a local climate effect (Chave et al., 2014, eq. 7). Soil phosphorus was from site-specific measurements (Condit et al., 2013; Turner and Condit, 2022). MCWD was calculated by Condit through spatial modeling of ground-based precipitation data (Condit et al., 2013; Turner and Condit, 2022). Symbols indicate stand-age class, as defined in Figure 2. Figure S3 presents an alternative version of this figure using MCWD calculated from monthly climatologies for precipitation and potential evapotranspiration from CHELSA v. 2.1 for the relevant 1-km grid cell (see Fig. 1; data from Karger et al., 2017, 2018) and using AGB and AWP calculated with an allometry that is invariant across sites. Other abbreviations are explained in Table 1.

to complement ground-based data collection (Bohlman, 2010; Schimel et al., 2019; chapter 52, Bohlman, 2024; chapter 50, Cushman, 2024).

These plots have served as foci for a variety of complementary data collection efforts, which offer additional opportunities to further investigate underlying mechanisms (Table 1). Other forest carbon stocks and fluxes have been measured in studies of soil carbon (Cusack et al., 2018), soil carbon dioxide efflux also known as soil respiration (Matson et al., 2017; Cusack et al., 2019), and litterfall (Cusack et al., 2018). A wide variety of plant functional traits have been measured on trees sampled from these plots, providing data on tree functional composition and enabling associated analyses (Umaña et al., 2021). Precise annual measurements of tree growth with dendrometers currently are being conducted on subsets of trees at 24 plots in the region, providing information on how annual climate variation affects tree growth and mortality. Tree heights have been measured on most of the dendrometer trees in the past decade, enabling tests for changes in tree allometries with environmental gradients (Ramos et al., 2024). Canopy imaging and photogrammetry using drones and associated mapping of crowns in the canopy has recently been expanded from BCI (Park et al., 2019; Araujo et al., 2021) to other plots in the region (Vasquez et al., 2024). Lianas (woody vines) are regularly censused at a subset of plots (Parolari et al., 2020); it is possible that variation in liana abundance plays a critical role in explaining among-plot variation in tree woody productivity and mortality (Ingwell et al., 2010). Seedlings are also regularly censused in a subset of plots, enabling investigation of how regeneration dynamics vary with climate and soils (Browne et al., 2021a, 2021b; Browne et al., 2022, 2023). Additional research focused on comparisons among just the large plots—Cocoli, Sherman, and BCI—including studies of deciduousness (Condit et al., 2000), tree allometries (Bohlman, personal communication), tree growth and mortality in response to an El Nino (Condit et al., 2004), and the role of tree size in forest carbon cycling (Meakem et al., 2018).

Future research at these regional plots should address enduring unknowns regarding the patterns and mechanisms of variation in tropical forest carbon stocks and fluxes. These include true patterns of variation in biomass and woody productivity (rather than those estimated using allometric equations), patterns and mechanisms of variation in woody residence time, and the roles of shifting plant functional composition, allocation patterns, and interactions with lianas and natural enemies in driving observed patterns. High-resolution terrestrial or drone laser scanning data are of particular interest for precisely and accurately quantifying wood volume, wood production, and wood turnover (including branchfall), without relying on assumptions about biomass allometries (Clark and Kellner, 2012). Because woody residence time depends strongly on mortality and branchfall rates of the largest trees, large sample sizes in area or time are required to quantify regional patterns precisely (Gora and Esquivel-Muelbert, 2022); this could be accomplished with drone or airborne remote sensing (Cushman et al., 2022). Additional site-level studies of other carbon stocks and fluxes could address how sites vary in production of leaves, roots, and plant reproductive material, in total net primary productivity (NPP, including all production of all tissues of all plants, not just wood production of trees), in autotrophic respiration (respiration by plants), and in gross primary productivity (GPP = NPP + autotrophic respiration), as in the GEM protocols (Malhi et al., 2021). This would make it possible to compare patterns of NPP and GPP with patterns of NPP and to test for shifts in NPP allocation and carbon use efficiency (NPP/GPP) across site. Quantification of root allocation, abundance, form, and function is of particular interest in relation to the strong regional gradients in soil nutrient availability. Direct measurements of soil moisture throughout the dry season would enable better characterization of among-site variation in water availability, which is influenced not only by climate but also by soil water-holding capacity and local topography.

Finally, an opportunity exists for greater integration among existing studies to enable enhanced synergies, including simply greater colocation of research activities in the same subsets of plots. Importantly, better integration among studies of trees, lianas, microbes, insects, and other animals could illuminate the role of interactions with natural enemies in driving shifts in tree functional composition, productivity, woody residence time, and biomass along these environmental gradients.

TABLE 1. Selected datasets collected in the central Panama plots and inventory sites.

Dataset	Description and methods (reference[a])	Plots[b]	Dataset contact (reference[a])
Tree census data	One or more censuses of all trees ≥10 cm dbh. In the case of 1-ha plots, most also have censuses of trees 1–10 cm dbh in a 0.16-ha subplot. (1)	All 67 plots	(2, 3)
Soil chemistry	Soil pH (in water and in CaCl2 solution), phosphorus (resin, Mehlich, total), nitrogen (ammonium, nitrate, total inorganic, dissolved organic, total), important elements (calcium, potassium, aluminum, iron, zinc, manganese, magnesium, boron), total bases, total carbon, and microbial carbon, nitrogen and phosphorus. (1)	42–45 plots, and up to 29–32 inventory sites, depending on the variable	(4)
Plant functional traits	Leaf, wood, and fruit functional trait collection on trees and lianas. (5)	bci, sherman, metrop, and others	S. Joseph Wright (6)
Dendrometers, subset	Annual measurements of band dendrometers on a size-stratified and spatially stratified subset of trees, since 2009–2013. (7)	bci, sherman, p05, p08, p18, p21, p22, p23, p24, p25, p26, p27, p28	Helene C. Muller-Landau (3)
Dendrometers, full	Annual measurements of band dendrometers on all trees with trunk diameter ≥ 10 cm, since 2018-2021 (many previously had dendrometers on a subset of trees). (7)	elcharco, fincaroubik gigante2, metrop, metrop2, p06, p09, p12, p14, p15, p16	Helene C. Muller-Landau (3)
Liana stem census	For 1-ha plots, stem census of all lianas ≥5 cm dbh in the entire 1-ha plot, and ≥1 cm dbh in a 40 × 40 m subplot (same one in which trees are measured in this size class) in 2010–2012. For BCI 50 ha plot, complete census of lianas ≥1 cm dbh. (8)	p01, p02, metrop, p05, p06, p07, p09, p15, elcharco, soberanía, bci	Stefan Schnitzer
Seedling census	Annual censuses of seedlings ≥200 mm in height and <1 cm dbh in 400 1-m^2 quadrats within each plot, since 2013 (except not panamapacifico in 2018 and not P15 in 2019 and 2020). (9, 10)	panamapacifico, metrop, soberanía, elcharco, p15, p12 sherman, fincaroubik	Liza Comita (11, 12)
Tree heights	One-time measurements of tree heights with laser rangefinders on dendrometer trees.	Dendrometer plots	Helene C. Muller-Landau (13)
Drone photogrammetry	High-resolution (3 cm) drone-acquired RGB imagery of the canopy, and mapping of crowns (>25 m^2) in the canopy, —one or more times through 2023.	Dendrometer plots	Helene C. Muller-Landau (14)
Airborne lidar	High-resolution (1 m) airborne lidar data, collected May 2023	bci, p14, p10, gigante1, gigante2, p12, sherman, metrop, p05, p06, p07, p15, p12, elcharco, soberanía, fincaroubik, panamapacifico	(15)
Litterfall, Wright	Long-term, ongoing, with weekly to monthly data collection depending on the site (also Poacher's peninsula on BCI).	bci, sherman, gigante fertilization	S. Joseph Wright
Litterfall, Cusack	Biweekly collection at 50 1 × 1 m traps for 1 year in 2013–2014. (16)	metro1, panamapacifico, p07, p12, elcharco, fincaroubik, sherman, soberania	Daniela F. Cusack (16)
Soil respiration, Corre	Measurements at 16 points per plot, every two to three weeks from June 2010 to February 2012. CH_4 and N_2O fluxes were also measured. (17)	metrop, p08, p19, p27, p32	Marife Corre
Soil respiration, Cusack	Measurements at 12 points per plot, one to three times in the dry season and one to three times in the wet season of 2015–2016. (18)	cerrogalera, albrook, metrop, soberania, elcharco, p25, p15, campochagres, bci, p13, p12, p04, sherman, p01, fincaroubik	Daniela F. Cusack

TABLE 1. (*Continued*).

Dataset	Description and methods (reference[a])	Plots[b]	Dataset contact (reference[a])
Soil carbon stocks to 1 m depth	Soil cores to 1-m depth (divided into four depth classes: 0–10, 10–20, 20–50, and 50–100 cm) at five points, and eight additional samples of surface soils (0–10 cm). (16)	albrook, bci, campochagres, cardenas, caritas, cerrogalera, cerropelado, coba1, coba2, elcharco, gigante1, gigante2, lp1, lp2, metrop, panamapacfico, p01–p28, p32, fincaroubik, sherman, soberania	Daniela F. Cusack (1)
Fine root biomass to 1 m depth	Oven-dried mass of live fine roots exhaustively removed from soil samples by hand for four depth classes (0–10, 10–20, 20–50, and 50–100 cm). Based on sampling to 1-m depth at five points per plot, and surface (0–10 cm) samples at eight more points. (19)	43 plots	Daniela F. Cusack (19)

[a] References:

1. Condit et al. (2013)
2. Condit et al. (2019)
3. ForestGEO (n.d.)
4. Turner and Condit (2022)
5. Wright et al. (2010)
6. Kattge et al. (2020)
7. Muller-Landau (2023)
8. Parolari et al., (2020)
9. Browne et al. (2021a)
10. Browne et al. (2023)
11. Browne et al. (2021b)
12. Browne et al. (2022)
13. Ramos et al. (2024)
14. Vasquez et al. (2024)
15. ForestGEO (2024)
16. Cusack et al. (2018)
17. Matson et al. (2017)
18. Cusack et al. (2019)
19. Cusack and Turner (2021)

[b] Plot identifiers (e.g., p05, elcharco) are codes used in the ForestGEO tree census datasets; “bci” is the Barro Colorado Island 50-ha plot; “sherman” is a 5.96-ha San Lorenzo plot that includes the San Lorenzo canopy crane; “metrop” is the 1-ha plot under the Parque Natural Metropolitano canopy crane. All other plots are 1 ha in area. The Barro Colorado Nature Monument sites are p10, p14, and bci on Barro Colorado Island; p11 and p18 on the Peña Blanca Peninsula; gigante1 and gigante2 on the Gigante Peninsula; and p12 and p13 on the Bohio Peninsula. The locations and environmental data on all plots are given in Table S1.

ACKNOWLEDGMENTS

We thank Ed Tanner and an anonymous reviewer for comments on an earlier version of this manuscript, and K. C. Cushman for contributing to the analyses presented in figures S1 and S2. We thank the many field and laboratory assistants who have measured trees, collected soil, run extractions, and entered data; Steve Dolins for designing the tree database; and Stuart Davies for overseeing the re-censuses in recent years. Funding for the tree census and soil chemistry data collection was provided by Smithsonian ForestGEO, the Smithsonian Tropical Research Institute, U.S. National Science Foundation Grant 0948585, the U.S. Department of Defense, the U.S. Agency for International Development, Conservation International’s Tropical Ecology Assessment and Monitoring (CI-TEAM) program, and the Deutsche Forschungsgemeinschaft. The BCI Forest Dynamics Research Project was made possible by National Science Foundation grants to Stephen P. Hubbell (DEB-0640386, DEB-0425651, DEB-0346488, DEB-0129874, DEB-00753102, DEB-9909347, DEB-9615226, DEB-9615226, DEB-9405933, DEB-9221033, DEB-9100058, DEB-8906869, DEB-8605042, DEB-8206992, DEB-7922197), support from the Forest Global Earth Observatory (ForestGEO), the Smithsonian Tropical Research Institute, the John D. and Catherine T. MacArthur Foundation, the Mellon Foundation, the Small World Institute Fund, and numerous private individuals.

AUTHOR CONTRIBUTIONS

H. M. conceived this study, designed the analyses, contributed to the implementation of the statistical analyses and figure preparation, and drafted the manuscript. C. P. led the statistical analyses and figure preparation, and provided input on the manuscript. R. P., S. A., and D. M. conducted botanical identifications and led the field teams. S. L. managed data. R. C. designed and set up the original plot network, obtained funding for the plot censuses, organized the plot censuses during his tenure at STRI, oversaw the design of the tree database, and managed data.

ONLINE SUPPLEMENTARY MATERIAL

Appendix S1. R code for running analyses. https://doi.org/10.25573/data.22798523

Table S1. Plot-level values of climate, soil, and forest carbon variables. https://doi.org/10.25573/data.22798586

Figures S1–S4. Supplemental figures. https://doi.org/10.25573/data.22798607

REFERENCES

Araujo, R. F., S. Grubinger, C. H. S. Celes, R. I. Negrón-Juárez, M. Garcia, J. P. Dandois, and H. C. Muller-Landau. 2021. Strong Temporal Variation in Treefall and Branchfall Rates in a Tropical Forest Is Related to Extreme Rainfall: Results from 5 Years of Monthly Drone Data for a 50-ha Plot. *Biogeosciences*, 18: 6517–6531. https://doi.org/10.5194/bg-18-6517-2021

Bohlman, S. A. 2010. Landscape Patterns and Environmental Controls of Deciduousness in Forests of Central PANAMA. *Global Ecology And Biogeography*, 19: 376–385. https://doi.org/10.1111/j.1466-8238.2009.00518.x

Bohlman, S. A. 2024. Remote Sensing of Tropical Forest Plant Composition, Diversity, and Function. In *The First 100 Years of Research on Barro Colorado: Plant and Ecosystem Science*, ed. H. C. Muller-Landau and S. J. Wright, pp. 465–472. Washington, D.C.: Smithsonian Institution Scholarly Press.

Browne, L., L. Markesteijn, B. M. J. Engelbrecht, F. A. Jones, O. T. Lewis, E. Manzane-Pinzon, S. J. Wright, and L. S. Comita. 2021a. Increased Mortality of Tropical Tree Seedlings During the Extreme 2015-16 El Niño. *Global Change Biology*, 27: 5043–5053. https://doi.org/10.1111/gcb.15809

Browne, L., L. Markesteijn, B. M. J. Engelbrecht, F. A. Jones, O. T. Lewis, E. Manzane-Pinzon, S. J. Wright, and L. S. Comita. 2021b. Increased Mortality of Tropical Tree Seedlings During the Extreme 2015-16 El Niño. Dataset. Figshare. https://doi.org/10.6084/m9.figshare.14204258.v1

Browne, L., L. Markesteijn, E. Manzane-Pinzon, S. J. Wright, R. Bagchi, B. M. J. Engelbrecht, F. A. Jones, and L. S. Comita. 2022. Widespread Variation in Functional Trait-Vital Rate Relationships in Tropical Tree Seedlings Across a Precipitation and Soil Phosphorus Gradient. Dataset. Dryad. https://doi.org/10.5061/dryad.mkkwh713s

Browne, L., L. Markesteijn, E. Manzane-Pinzon, S. J. Wright, R. Bagchi, B. M. J. Engelbrecht, F. A. Jones, and L. S. Comita. 2023. Widespread Variation in Functional Trait-Vital Rate Relationships in Tropical Tree Seedlings Across a Precipitation and Soil Phosphorus Gradient. *Functional Ecology*, 37: 248–260. https://doi.org/10.1111/1365-2435.14213

Chave, J., R. Condit, S. Aguilar, A. Hernandez, S. Lao, and R. Pérez. 2004. Error Propagation and Scaling for Tropical Forest Biomass Estimates. *Philosophical Transactions of the Royal Society of London Series B: Biological Sciences*, 359: 409–420. https://doi.org/10.1098/rstb.2003.1425

Chave, J., M. Rejou-Mechain, A. Burquez, E. Chidumayo, M. S. Colgan, W. B. C. Delitti, A. Duque, T. Eid, P. M. Fearnside, R. C. Goodman, M. Henry, A. Martinez-Yrizar, W. A. Mugasha, H. C. Muller-Landau, M. Mencuccini, B. W. Nelson, A. Ngomanda, E. M. Nogueira, E. Ortiz-Malavassi, R. Pelissier, P. Ploton, C. M. Ryan, J. G. Saldarriaga, and G. Vieilledent. 2014. Improved Allometric Models to Estimate the Aboveground Biomass of Tropical Trees. *Global Change Biology*, 20: 3177–3190. https://doi.org/10.1111/gcb.12629

Clark, D. B., and J. R. Kellner. 2012. Tropical forest Biomass Estimation and the Fallacy of Misplaced Concreteness. *Journal of Vegetation Science*, 23: 1191–1196.

Cleveland, C. C., A. R. Townsend, P. Taylor, S. Alvarez-Clare, M. M. Bustamante, G. Chuyong, S. Z. Dobrowski, P. Grierson, K. E. Harms, B. Z. Houlton, A. Marklein, W. Parton, S. Porder, S. C. Reed, C. A. Sierra, W. L. Silver, E. V. Tanner, and W. R. Wieder. 2011. Relationships Among Net Primary Productivity, Nutrients and Climate in Tropical Rain Forest: A Pan-Tropical Analysis. *Ecology Letters*, 14: 939–947. https://doi.org/10.1111/j.1461-0248.2011.01658.x

Condit, R. 2024. Tree Species Composition of Barro Colorado Island in a Wider Context: The Canal Area and the Nation of Panama. In *The First 100 Years of Research on Barro Colorado: Plant and Ecosystem Science*, ed. H. C. Muller-Landau and S. J. Wright, pp. 79–87. Washington, D.C.: Smithsonian Institution Scholarly Press.

Condit, R., S. Aguilar, A. Hernandez, R. Pérez, S. Lao, G. Angehr, S. P. Hubbell, and R. B. Foster. 2004. Tropical forest Dynamics Across a Rainfall Gradient and the Impact of an El Nino Dry Season. *Journal of Tropical Ecology*, 20: 51–72.

Condit, R., B. M. J. Engelbrecht, D. Pino, R. Pérez, and B. L. Turner. 2013. Species Distributions in Response to Individual Soil Nutrients and Seasonal Drought Across a Community of Tropical Trees. *Proceedings of the National Academy of Sciences of the United States Of America*, 110: 5064–5068. https://doi.org/10.1073/pnas.1218042110

Condit, R., R. Pérez, S. Aguilar, and S. Lao. 2019. Census Data from 65 Tree Plots in Panama, 1994–2015. https://doi.org/10.15146/mdpr-pm59

Condit, R., N. Pitman, E. G. Leigh, Jr., J. Chave, J. Terborgh, R. B. Foster, P. Núñez, H. Vargas, S. Aguilar, R. Valencia, G. Villa, H. Muller-Landau, E. Losos, and S. P. Hubbell. 2002. Beta-Diversity in Tropical Forest Trees. *Science*, 295: 666–669.

Condit, R., W. D. Robinson, R. Ibáñez, S. Aguilar, A. Sanjur, R. Martínez, R. F. Stallard, T. García, G. R. Angehr, and L. Petit. 2001. The Status of the Panama Canal Watershed and Its Biodiversity at the Beginning of the 21st Century Long-term Ecological Studies Reveal a Diverse Flora and Fauna Near the Panama Canal, Harbored Within a Corridor of Forest Stretching from the Caribbean to the Pacific, but Deforestation, Land Degradation, Erosion, and Overhunting Remain Threats. *BioScience*, 51: 389–398.

Condit, R., K. Watts, S. A. Bohlman, R. Pérez, R. B. Foster, and S. P. Hubbell. 2000. Quantifying the Deciduousness of Tropical Forest Canopies Under Varying Climates. *Journal of Vegetation Science*, 11: 649–658.

Cusack, D. F. 2024. Mechanisms and Patterns of Soil Carbon Storage and Cycling in the Barro Colorado Nature Monument, Panama. In *The First 100 Years of Research on Barro Colorado: Plant and Ecosystem Science*, ed. H. C. Muller-Landau and S. J. Wright, pp. 505–517. Washington, D.C.: Smithsonian Institution Scholarly Press.

Cusack, D. F., D. Ashdown, L. H. Dietterich, A. Neupane, M. Ciochina, and B. L. Turner. 2019. Seasonal Changes in Soil Respiration Linked to Soil Moisture and Phosphorus Availability Along a Tropical Rainfall Gradient. *Biogeochemistry*, 145: 235–254. https://doi.org/10.1007/s10533-019-00602-4

Cusack, D. F., L. Markesteijn, R. Condit, O. T. Lewis, and B. L. Turner. 2018. Soil Carbon Stocks Across Tropical Forests of Panama Regulated by Base Cation Effects on Fine Roots. *Biogeochemistry*, 137: 253–266. https://doi.org/10.1007/s10533-017-0416-8

Cusack, D. F., and B. L. Turner. 2021. Fine Root and Soil Organic Carbon Depth Distributions are Inversely Related Across Fertility and Rainfall Gradients in Lowland Tropical Forests. *Ecosystems*, 24: 1075–1092. https://doi.org/10.1007/s10021-020-00569-6

Cushman, K. C. 2024. Remote Sensing of Forest Structure and Dynamics in the Barro Colorado Nature Monument. In *The First 100 Years of Research on Barro Colorado: Plant and Ecosystem Science*, ed. H. C. Muller-Landau and S. J. Wright, pp. 447–455. Washington, D.C.: Smithsonian Institution Scholarly Press.

Cushman, K. C., M. Detto, M. García, and H. C. Muller-Landau. 2022. Soils and Topography Control Natural Disturbance Rates and Thereby Forest Structure in a Lowland Tropical Landscape. *Ecology Letters*, 25: 1126–1138. https://doi.org/10.1111/ele.13978

Dalling, J. W., and B. L. Turner, eds. 2021. *Fortuna Forest Reserve, Panama: Interacting Effects of Climate and Soils on the Biota of a Wet Premontane Tropical Forest*. Smithsonian Contributions to Botany, No. 112. Washington, D.C.: Smithsonian Institution Scholarly Press. https://doi.org/10.5479/si.14315990

Engelbrecht, B. M. J., L. S. Comita, R. Condit, T. A. Kursar, M. T. Tyree, B. L. Turner, and S. P. Hubbell. 2007. Drought Sensitivity Shapes Species Distribution Patterns in Tropical Forests. *Nature*, 447: 80–82. https://doi.org/10.1038/nature05747

ForestGEO. n.d. ForestGEO Data Portal. Accessed May 15, 2023. http://ctfs.si.edu/datarequest/

ForestGEO, S. 2024. 2023 high-resolution airborne lidar data for Barro Colorado Island and other Smithsonian ForestGEO sites in Central Panama. Smithsonian Tropical Research Institute. Dataset. https://doi.org/10.25573/data.24955347

Gora, E. M., and A. Esquivel-Muelbert. 2021. Implications of size-dependent tree mortality for tropical forest carbon dynamics. *Nature Plants*, 7: 384–391. https://doi.org/10.1038/s41477-021-00879-0

Ingwell, L. L., S. J. Wright, K. K. Becklund, S. P. Hubbell, and S. A. Schnitzer. 2010. The Impact of Lianas on 10 Years of Tree Growth and Mortality on Barro Colorado Island, Panama. *Journal of Ecology*, 98: 879–887. https://doi.org/10.1111/j.1365-2745.2010.01676.x

Karger, D. N., O. Conrad, J. Böhner, T. Kawohl, H. Kreft, R. W. Soria-Auza, N. E. Zimmermann, P. Linder, and M. Kessler. 2017. Climatologies at High Resolution for the Earth Land Surface Areas. *Scientific Data*, 4: 170122. https://doi.org/10.1038/sdata.2017.122

Karger, D. N., O. Conrad, J. Böhner, T. Kawohl, H. Kreft, R. W. Soria-Auza, N. E. Zimmermann, H. P. Linder, and M. Kessler. 2018. Data from: Climatologies at high resolution for the earth's land surface areas. *EnviDat*. https://doi.org/10.16904/envidat.228.v2.1

Kattge, J., G. Boenisch, S. Diaz, S. Lavorel, I. C. Prentice, P. Leadley, S. Tautenhahn, G. D. A. Werner, T. Aakala, M. Abedi, A. T. R. Acosta, G. C. Adamidis, K. Adamson, M. Aiba, C. H. Albert, J. M. Alcantara, C. C. Alcazar, I. Aleixo, H. Ali, B. Amiaud, C. Ammer, M. M. Amoroso, M. Anand, C. Anderson, N. Anten, J. Antos, D. M. G. Apgaua, T.-L. Ashman, D. H. Asmara, G. P. Asner, M. Aspinwall, O. Atkin, I. Aubin, L. Baastrup-Spohr, K. Bahalkeh, M. Bahn, T. Baker, W. J. Baker, J. P. Bakker, D. Baldocchi, J. Baltzer, A. Banerjee, A. Baranger, J. Barlow, D. R. Barneche, Z. Baruch, D. Bastianelli, J. Battles, W. Bauerle, M. Bauters, E. Bazzato, M. Beckmann, H. Beeckman, C. Beierkuhnlein, R. Bekker, G. Belfry, M. Belluau, M. Beloiu, R. Benavides, L. Benomar, M. L. Berdugo-Lattke, E. Berenguer, R. Bergamin, J. Bergmann, M. B. Carlucci, L. Berner, M. Bernhardt-Roemermann, C. Bigler, A. D. Bjorkman, C. Blackman, C. Blanco, B. Blonder, D. Blumenthal, K. T. Bocanegra-Gonzalez, P. Boeckx, S. Bohlman, K. Boehning-Gaese, L. Boisvert-Marsh, W. Bond, B. Bond-Lamberty, A. Boom, C. C. F. Boonman, K. Bordin, E. H. Boughton, V. Boukili, D. M. J. S. Bowman, S. Bravo, M. R. Brendel, M. R. Broadley, K. A. Brown, H. Bruelheide, F. Brumnich, H. H. Bruun, D. Bruy, S. W. Buchanan, S. F. Bucher, N. Buchmann, R. Buitenwerf, D. E. Bunker, J. Buerger, S. Burrascano, D. F. R. P. Burslem, B. J. Butterfield, C. Byun, M. Marques, M. C. Scalon, M. Caccianiga, M. Cadotte, M. Cailleret, J. Camac, J. Julio Camarero, C. Campany, G. Campetella, J. A. Campos, L. Cano-Arboleda, R. Canullo, M. Carbognani, F. Carvalho, F. Casanoves, B. Castagneyrol, J. A. Catford, J. Cavender-Bares, B. E. L. Cerabolini, M. Cervellini, E. Chacon-Madrigal, K. Chapin, F. S. Chapin, S. Chelli, S.-C. Chen, A. Chen, P. Cherubini, F. Chianucci, B. Choat, K.-S. Chung, M. Chytry, D. Ciccarelli, L. Coll, C. G. Collins, L. Conti, D. Coomes, J. H. C. Cornelissen, W. K. Cornwell, P. Corona, M. Coyea, J. Craine, D. Craven, J. P. G. M. Cromsigt, A. Csecserits, K. Cufar, M. Cuntz, A. C. da Silva, K. M. Dahlin, M. Dainese, I. Dalke, M. Dalle Fratte, D.-L. Anh Tuan, J. Danihelka, M. Dannoura, S. Dawson, A. J. de Beer, A. De Frutos, J. R. De Long, B. Dechant, S. Delagrange, N. Delpierre, G. Derroire, A. S. Dias, M. H. Diaz-Toribio, P. G. Dimitrakopoulos, M. Dobrowolski, D. Doktor, P. Drevojan, N. Dong, J. Dransfield, S. Dressler, L. Duarte, E. Ducouret, S. Dullinger, W. Durka, R. Duursma, O. Dymova, A. E-Vojtko, R. L. Eckstein, H. Ejtehadi, J. Elser, T. Emilio, K. Engemann, M. B. Erfanian, A. Erfmeier, A. Esquivel-Muelbert, G. Esser, M. Estiarte, T. F. Domingues, W. F. Fagan, J. Fagundez, D. S. Falster, Y. Fan, J. Fang, E. Farris, F. Fazlioglu, Y. Feng, F. Fernandez-Mendez, C. Ferrara, J. Ferreira, A. Fidelis, B. Finegan, J. Firn, T. J. Flowers, D. F. B. Flynn, V. Fontana, E. Forey, C. Forgiarini, L. Francois, M. Frangipani, D. Frank, C. Frenette-Dussault, G. T. Freschet, E. L. Fry, N. M. Fyllas, G. G. Mazzochini, S. Gachet, R. Gallagher, G. Ganade, F. Ganga, P. Garcia-Palacios, V. Gargaglione, E. Garnier, J. Luis Garrido, A. Luis de Gasper, G. Gea-Izquierdo, D. Gibson, A. N. Gillison, A. Giroldo, M.-C. Glasenhardt, S. Gleason, M. Gliesch, E. Goldberg, B. Goeldel, E. Gonzalez-Akre, J. L. Gonzalez-Andujar, A. Gonzalez-Melo, A. Gonzalez-Robles, B. J. Graae, E. Granda, S. Graves, W. A. Green, T. Gregor, N. Gross, G. R. Guerin, A. Guenther, A. G. Gutierrez, L. Haddock, A. Haines, J. Hall, A. Hambuckers, W. Han, S. P. Harrison, W. Hattingh, J. E. Hawes, T. He, P. He, J. M. Heberling, A. Helm, S. Hempel, J. Hentschel, B. Herault, A.-M. Heres, K. Herz, M. Heuertz, T. Hickler, P. Hietz, P. Higuchi, A. L. Hipp, A. Hirons, M. Hock, J. A. Hogan, K. Holl, O. Honnay, D. Hornstein, E. Hou, N. Hough-Snee, K. A. Hovstad, T. Ichie, B. Igic, E. Illa, M. Isaac, M. Ishihara, L. Ivanov, L. Ivanova, C. M. Iversen, J. Izquierdo, R. B. Jackson, B. Jackson, H. Jactel, A. M. Jagodzinski, U. Jandt, S. Jansen, T. Jenkins, A. Jentsch, J. R. P. Jespersen, G.-F. Jiang, J. L. Johansen, D. Johnson, E. J. Jokela, C. A. Joly, G. J. Jordan, G. S. Joseph, D. Junaedi, R. R. Junker, E. Justes, R. Kabzems, J. Kane, Z. Kaplan, T. Kattenborn, L. Kavelenova, E. Kearsley, A. Kempel, T. Kenzo, A. Kerkhoff, M. I. Khalil, N. L. Kinlock, W. D. Kissling, K. Kitajima, T. Kitzberger, R. Kjoller, T. Klein, M. Kleyer, J. Klimesova, J. Klipel, B. Kloeppel, S. Klotz, J. M. H. Knops, T. Kohyama, F. Koike, J. Kollmann, B. Komac, K. Komatsu, C. Koenig, N. J. B. Kraft, K. Kramer, H. Kreft, I. Kuehn, D. Kumarathunge, J. Kuppler, H. Kurokawa, Y. Kurosawa, S. Kuyah, J.-P. Laclau, B. Lafleur, E. Lallai, E. Lamb, A. Lamprecht, D. J. Larkin, D. Laughlin, Y. Le Bagousse-Pinguet, G. le Maire, P. C. le Roux, E. le Roux, T. Lee, F. Lens, S. L. Lewis, B. Lhotsky, Y. Li, X. Li, J. W. Lichstein, M. Liebergesell, J. Y. Lim, Y.-S. Lin, J. C. Linares, C. Liu, D. Liu, U. Liu, S. Livingstone, J. Llusia, M. Lohbeck, A. Lopez-Garcia, G. Lopez-Gonzalez, Z. Lososova, F. Louault, B. A. Lukacs, P. Lukes, Y. Luo, M. Lussu, S. Ma, C. M. R. Pereira, M. Mack, V. Maire, A. Makela, H. Makinen, A. C. Mendes Malhado, A. Mallik, P. Manning, S. Manzoni, Z. Marchetti, L. Marchino, V. Marcilio-Silva, E. Marcon, M. Marignani, L. Markesteijn, A. Martin, C. Martinez-Garza, J. Martinez-Vilalta, T. Maskova, K. Mason, N. Mason, T. J. Massad, J. Masse, I. Mayrose, J. McCarthy, M. L. McCormack, K. McCulloh, I. R. McFadden, B. J. McGill, M. Y. McPartland, J. S. Medeiros, B. Medlyn, P. Meerts, Z. Mehrabi, P. Meir, F. P. L. Melo, M. Mencuccini, C. Meredieu, J. Messier, I. Meszaros, J. Metsaranta, S. T. Michaletz, C. Michelaki, S. Migalina, R. Milla, J. E. D. Miller, V. Minden, R. Ming, K. Mokany, A. T. Moles, A. V. Molnar, J. Molofsky, M. Molz, R. A. Montgomery, A. Monty, L. Moravcova, A. Moreno-Martinez, M. Moretti, A. S. Mori, S. Mori, D. Morris, J. Morrison, L. Mucina, S. Mueller, C. D. Muir, S. C. Mueller, F. Munoz, I. H. Myers-Smith, R. W. Myster, M. Nagano, S. Naidu, A. Narayanan, B. Natesan, L. Negoita, A. S. Nelson, E. L. Neuschulz, J. Ni, G. Niedrist, J. Nieto, U. Niinemets, R. Nolan, H. Nottebrock, Y. Nouvellon, A. Novakovskiy, K. O. Nystuen, A. O'Grady, K. O'Hara, A. O'Reilly-Nugent, S. Oakley, W. Oberhuber, T. Ohtsuka, R. Oliveira, K. Ollerer, M. E. Olson, V. Onipchenko, Y. Onoda, R. E. Onstein, J. C. Ordonez, N. Osada, I. Ostonen, G. Ottaviani, S. Otto, G. E. Overbeck, W. A. Ozinga, A. T. Pahl, C. E. T. Paine, R. J. Pakeman, A. C. Papageorgiou, E. Parfionova, M. Paertel, M. Patacca, S. Paula, J. Paule, H. Pauli, J. G. Pausas, B. Peco, J. Penuelas, A. Perea, P. Luis Peri, A. C. Petisco-Souza, A. Petraglia, A. M. Petritan, O. L. Phillips, S. Pierce, V. D. Pillar, J. Pisek, A. Pomogaybin, H. Poorter, A. Portsmuth, P. Poschlod, C. Potvin, D. Pounds, A. S. Powell, S. A. Power, A. Prinzing, G. Puglielli, P. Pysek, V. Raevel, A. Rammig, J. Ransijn, C. A. Ray, P. B. Reich, M. Reichstein, D. E. B. Reid, M. Rejou-Mechain, V. Resco de Dios, S. Ribeiro, S. Richardson, K. Riibak, M. C. Rillig, F. Riviera, E. M. R. Robert, S. Roberts, B. Robroek, A. Roddy, A. V. Rodrigues, A. Rogers, E. Rollinson, V. Rolo, C. Roemermann, D. Ronzhina, C. Roscher, J. A. Rosell, M. F. Rosenfield, C. Rossi, D. B. Roy, S. Royer-Tardif, N. Rueger, R. Ruiz-Peinado, S. B. Rumpf, G. M. Rusch, M. Ryo, L. Sack, A. Saldana, B. Salgado-Negret, R. Salguero-Gomez, I. Santa-Regina, A. Carolina Santacruz-Garcia, J. Santos, J. Sardans, B. Schamp, M. Scherer-Lorenzen, M. Schleuning, B. Schmid, M. Schmidt, S. Schmitt, J. V. Schneider, S. D. Schowanek, J. Schrader, F. Schrodt, B. Schuldt, F. Schurr, G. Selaya Garvizu, M. Semchenko, C. Seymour, J. C. Sfair, J. M. Sharpe, C. S. Sheppard, S. Sheremetiev, S. Shiodera, B. Shipley, T. A. Shovon, A. Siebenkaes, S. Carlos, V. Silva, M. Silva, T. Sitzia, H. Sjoman, M. Slot, N. G. Smith, D. Sodhi, P. Soltis, D. Soltis, B. Somers, G. Sonnier, M. V. Sorensen, E. E. Sosinski, Jr., N. A. Soudzilovskaia, A. F. Souza, M. Spasojevic, M. G. Sperandii, A. B. Stan, J. Stegen, K. Steinbauer, J. G. Stephan, F. Sterck, D. B. Stojanovic, T. Strydom, M. Laura Suarez, J.-C. Svenning, I. Svitkova, M. Svitok, M. Svoboda, E. Swaine, N. Swenson, M. Tabarelli, K. Takagi, U. Tappeiner, R. Tarifa, S. Tauugourdeau, C. Tavsanoglu, M. te Beest, L. Tedersoo, N. Thiffault, D. Thom, E. Thomas, K. Thompson, P. E. Thornton, W. Thuiller, L. Tichy, D. Tissue, M. G. Tjoelker, D. Y. P. Tng, J. Tobias, P. Torok, T. Tarin, J. M. Torres-Ruiz, B. Tothmeresz, M. Treurnicht, V. Trivellone, F. Trolliet, V. Trotsiuk, J. L. Tsakalos, I. Tsiripidis, N. Tysklind, T. Umehara, V. Usoltsev, M. Vadeboncoeur, J. Vaezi, F. Valladares, J. Vamosi, P. M. van Bodegom, M. van Breugel, E. Van Cleemput, M. van de Weg, S. van der Merwe, F. van der Plas, M. T. van der Sande, M. van Kleunen, K. Van Meerbeek, M. Vanderwel, K. A. Vanselow, A. Varhammar, L. Varone, M. Y. Vasquez Valderrama, K. Vassilev, M. Vellend, E. J. Veneklaas, H. Verbeeck, K. Verheyen, A. Vibrans, I. Vieira, J. Villacis, C. Violle, P. Vivek, K. Wagner, M. Waldram, A. Waldron, A. P. Walker, M. Waller, G. Walther, H. Wang, F. Wang, W. Wang, H. Watkins, J. Watkins, U. Weber, J. T. Weedon, L. Wei, P. Weigelt, E. Weiher, A. W. Wells, C. Wellstein, E. Wenk, M. Westoby, A. Westwood, P. J. White, M. Whitten, M. Williams, D. E. Winkler, K. Winter, C. Womack, I. J. Wright, S. J. Wright, J. Wright, B. X. Pinho, F. Ximenes, T. Yamada, K. Yamaji, R. Yanai, N. Yankov, B. Ygeul, K. J. Zanini, A. E. Zanne, D. Zeleny, Y.-P. Zhao, J. Zheng, J. Zheng, K. Zieminska, C. R. Zirbel, G. Zizka, I. C. Zo-Bi, G. Zotz, C. Wirth, and N. Nutrient. 2020. TRY Plant Trait Database: Enhanced Coverage and Open Access. *Global Change Biology*, 26: 119–188. https://doi.org/10.1111/gcb.14904

Kohyama, T. S., T. I. Kohyama, and D. Sheil. 2018. Definition and Estimation of Vital Rates from Repeated Censuses: Choices, Comparisons and Bias Corrections Focusing on Trees. *Methods in Ecology and Evolution*, 9: 809–821. https://doi.org/doi:10.1111/2041-210X.12929

Malhi, Y., C. Girardin, D. B. Metcalfe, C. E. Doughty, L. E. O. C. Aragão, S. W. Rifai, I. Oliveras, A. Shenkin, J. Aguirre-Gutiérrez, C. A. L. Dahlsjö, T. Riutta, E. Berenguer, S. Moore, W. H. Huasco, N. Salinas, A. C. L. da Costa, L. P. Bentley, S. Adu-Bredu, T. R. Marthews, P. Meir, and O. L. Phillips. 2021. The Global Ecosystems Monitoring Network: Monitoring Ecosystem Productivity and Carbon Cycling Across the Tropics. *Biological Conservation*, 253: 108889. https://doi.org/10.1016/j.biocon.2020.108889

Mateo-Vega, J., J. P. Arroyo-Mora, and C. Potvin. 2019. Tree Aboveground Biomass and Species Richness of the Mature Tropical Forests of Darien, Panama, and Their Role in Global Climate Change Mitigation and Biodiversity Conservation. *Conservation Science and Practice*, 1: e42. https://doi.org/10.1111/csp2.42

Matson, A. L., M. D. Corre, K. Langs, and E. Veldkamp. 2017. Soil Trace Gas Fluxes Along Orthogonal Precipitation and Soil Fertility Gradients in Tropical Lowland Forests of Panama. *Biogeosciences*, 14: 3509–3524. https://doi.org/10.5194/bg-14-3509-2017

McDowell, N., C. D. Allen, K. Anderson-Teixeira, P. Brando, R. Brienen, J. Chambers, B. Christoffersen, S. Davies, C. Doughty, A. Duque, F. Espirito-Santo, R. Fisher, C. G. Fontes, D. Galbraith, D. Goodsman, C. Grossiord, H. Hartmann, J. Holm, D. J. Johnson, A. R. Kassim, M. Keller, C. Koven, L. Kueppers, T. o. Kumagai, Y. Malhi, S. M. McMahon, M. Mencuccini, P. Meir, P. Moorcroft, H. C. Muller-Landau, O. L. Phillips, T. Powell, C. A. Sierra, J. Sperry, J. Warren, C. Xu, and X. Xu. 2018. Drivers and Mechanisms of Tree Mortality in Moist Tropical Forests. *New Phytologist*, 219: 851–869. https://doi.org/10.1111/nph.15027

Meakem, V., A. J. Tepley, E. B. Gonzalez-Akre, V. Herrmann, H. C. Muller-Landau, S. J. Wright, S. P. Hubbell, R. Condit, and K. J. Anderson-Teixeira. 2018. Role of Tree Size in Moist Tropical Forest Carbon Cycling and Water Deficit Responses. *New Phytologist*, 219: 947–958. https://doi.org/10.1111/nph.14633

Muller-Landau, H. C. 2023. Combined Band Dendrometer Protocol Used by ForestGEO in Panama. Smithsonian Tropical Research Institute. Online resource. https://doi.org/10.25573/data.20010176

Muller-Landau, H. C., K. C. Cushman, E. E. Arroyo, I. Martinez Cano, K. J. Anderson-Teixeira, and B. Backiel. 2021. Patterns and Mechanisms of Spatial Variation in Tropical Forest Productivity, Woody Residence Time, and Biomass. *New Phytologist*, 229: 3065–3087. https://doi.org/10.1111/nph.17084

Muller-Landau, H. C., M. Detto, R. A. Chisholm, S. P. Hubbell, and R. Condit. 2014. Detecting and Projecting Changes in Forest Biomass from Plot Data. In *Forests and Global Change*, ed. D. A. Coomes and D. F. R. P. Burslem, pp. 381–415. Cambridge, U.K.: Cambridge University Press. https://doi.org/10.1017/CBO9781107323506.018

Park, J. Y., H. C. Muller-Landau, J. W. Lichstein, S. W. Rifai, J. P. Dandois, and S. A. Bohlman. 2019. Quantifying Leaf Phenology of Individual Trees and Species in a Tropical Forest Using Unmanned Aerial Vehicle (UAV) Images. *Remote Sensing*, 11: 1534. https://doi.org/10.3390/rs11131534

Parolari, A. J., K. Paul, A. Griffing, R. Condit, R. Pérez, S. Aguilar, and S. A. Schnitzer. 2020. Liana Abundance and Diversity Increase with Rainfall Seasonality Along a Precipitation Gradient in Panama. *Ecography*, 43: 25–33. https://doi.org/10.1111/ecog.04678

Pyke, C. R., R. Condit, S. Aguilar, and S. Lao. 2001. Floristic Composition Across a Climatic Gradient in a Neotropical Lowland Forest. *Journal of Vegetation Science*, 12: 553–566.

Quesada, C. A., J. Lloyd, M. Schwarz, S. Patiño, T. R. Baker, C. Czimczik, N. M. Fyllas, L. Martinelli, G. B. Nardoto, J. Schmerler, A. J. B. Santos, M. G. Hodnett, R. Herrera, F. J. Luizão, A. Arneth, G. Lloyd, N. Dezzeo, I. Hilke, I. Kuhlmann, M. Raessler, W. A. Brand, H. Geilmann, J. O. Moraes Filho, F. P. Carvalho, R. N. Araujo Filho, J. E. Chaves, O. F. Cruz Junior, T. P. Pimentel, and R. Paiva. 2010. Variations in Chemical and Physical Properties of Amazon Forest Soils in Relation to Their Genesis. *Biogeosciences*, 7: 1515–1541. https://doi.org/10.5194/bg-7-1515-2010

Ramos, P., P. Villareal, and H. C. Muller-Landau. 2024. Tree height measurements on Panama ForestGEO dendrometer trees. Smithsonian Tropical Research Institute. Dataset. https://doi.org/10.25573/data.24954204

Schimel, D., F. D. Schneider, J. P. L. Carbon, and P. Ecosystem. 2019. Flux towers in the Sky: Global Ecology from Space. *New Phytologist*, 224: 570–584. https://doi.org/10.1111/nph.15934

Turner, B. L., T. Brenes-Arguedas, and R. Condit. 2018. Pervasive Phosphorus Limitation of Tree Species but Not Communities in Tropical Forests. *Nature*, 555: 367–370. https://doi.org/10.1038/nature25789

Turner, B. L., and R. Condit. 2022. Soil Chemistry and Dry Season Intensity, Panama Canal Area. https://doi.org/10.7291/D1B963

Umaña, M. N., R. Condit, R. Pérez, B. L. Turner, S. J. Wright, and L. S. Comita. 2021. Shifts in Taxonomic and Functional Composition of Trees Along Rainfall and Phosphorus Gradients in Central Panama. *Journal of Ecology*, 109: 51–61. https://doi.org/10.1111/1365-2745.13442

van Breugel, M., D. Craven, H. R. Lai, M. Baillon, B. L. Turner, and J. S. Hall. 2019. Soil Nutrients and Dispersal Limitation Shape Compositional Variation in Secondary Tropical Forests Across Multiple Scales. *Journal of Ecology*, 107: 566–581. https://doi.org/10.1111/1365-2745.13126

Vasquez, V., M. Garcia, and H. C. Muller-Landau. 2024. Smithsonian ForestGEO San Lorenzo and Panama Small Plots aerial photogrammetry orthomosaics and digital surface models for 2015-2023. Smithsonian Tropical Research Institute. Dataset. https://doi.org/10.25573/data.24955356

Wang, L., W. P. Sousa, P. Gong, and G. S. Biging. 2004. Comparison of IKONOS and QuickBird Images for Mapping Mangrove Species on the Caribbean Coast of Panama. *Remote Sensing of Environment*, 91: 432–440. https://doi.org/10.1016/j.rse.2004.04.005

Woodring, W., R. Stewart, and J. Stewart. 1980. Geologic Map of the Panama Canal. Reston, VA: U.S. Geological Survey

Wright, S. J., K. E. Harms, O. Hernández, M. N. Garcia, and J. B. Yavitt. 2024. A Factorial Nitrogen, Phosphorus, and Potassium Addition Experiment Conducted in a Mature Lowland Tropical Forest in the Barro Colorado Nature Monument. In *The First 100 Years of Research on Barro Colorado: Plant and Ecosystem Science*, ed. H. C. Muller-Landau and S. J. Wright, pp. 539–547. Washington, D.C.: Smithsonian Institution Scholarly Press.

Wright, S. J., K. Kitajima, N. J. B. Kraft, P. B. Reich, I. J. Wright, D. E. Bunker, R. Condit, J. W. Dalling, S. J. Davies, S. Diaz, B. M. J. Engelbrecht, K. E. Harms, S. P. Hubbell, C. O. Marks, M. C. Ruiz-Jaen, C. M. Salvador, and A. E. Zanne. 2010. Functional Traits and the Growth-Mortality Trade-Off in Tropical Trees. *Ecology*, 91: 3664–3674. https://doi.org/10.1890/09-2335.1

Wright, S. J., B. L. Turner, J. B. Yavitt, K. E. Harms, M. Kaspari, E. V. J. Tanner, J. Bujan, E. A. Griffin, J. R. Mayor, S. C. Pasquini, M. Sheldrake, and M. N. Garcia. 2018. Plant Responses to Fertilization Experiments in Lowland, Species-Rich, Tropical Forests. *Ecology*, 99: 1129–1138. https://doi.org/10.1002/ecy.2193

Xu, L., S. Saatchi Sassan, Y. Yang, Y. Yu, J. Pongratz, A. A. Bloom, K. Bowman, J. Worden, J. Liu, Y. Yin, G. Domke, E. McRoberts Ronald, C. Woodall, G.-J. Nabuurs, S. de-Miguel, M. Keller, N. Harris, S. Maxwell, and D. Schimel. 2021. Changes in Global Terrestrial Live Biomass Over the 21st Century. *Science Advances*, 7: eabe9829. https://doi.org/10.1126/sciadv.abe9829